



UNIVERSITY OF LEEDS

This is a repository copy of *Effect of Nanoscale Confinement on the Crystallization of Potassium Ferrocyanide*.

White Rose Research Online URL for this paper:

<https://eprints.whiterose.ac.uk/104873/>

Version: Accepted Version

Article:

Anduix- Claro, C orcid.org/0000-0001-7156-4901, Kim, YY orcid.org/0000-0002-8503-4554, Wang, Y et al. (3 more authors) (2016) Effect of Nanoscale Confinement on the Crystallization of Potassium Ferrocyanide. *Crystal Growth and Design*, 16 (9). pp. 5403-5411. ISSN 1528-7483

<https://doi.org/10.1021/acs.cgd.6b00894>

© 2016, American Chemical Society. This document is the unedited author's version of a Submitted Work that was subsequently accepted for publication in *Crystal Growth and Design*, copyright © American Chemical Society after peer review. To access the final edited and published work, see <http://dx.doi.org/10.1021/acs.cgd.6b00894>.

Reuse

Items deposited in White Rose Research Online are protected by copyright, with all rights reserved unless indicated otherwise. They may be downloaded and/or printed for private study, or other acts as permitted by national copyright laws. The publisher or other rights holders may allow further reproduction and re-use of the full text version. This is indicated by the licence information on the White Rose Research Online record for the item.

Takedown

If you consider content in White Rose Research Online to be in breach of UK law, please notify us by emailing eprints@whiterose.ac.uk including the URL of the record and the reason for the withdrawal request.



eprints@whiterose.ac.uk
<https://eprints.whiterose.ac.uk/>

Effect of Nanoscale Confinement on the Crystallization of Potassium Ferrocyanide

Clara Anduix-Canto¹, Yi-Yeoun Kim¹, Yunwei Wang¹, Alex N. Kulak¹, Fiona C. Meldrum^{1†}
and Hugo K. Christenson^{2*}

¹School of Chemistry, University of Leeds, Woodhouse Lane, Leeds, LS2 9JT, UK.

²School of Physics and Astronomy, University of Leeds, Leeds, LS2 9JT, UK.

ABSTRACT

Many crystallization processes of great significance in nature and technology occur in small volumes rather than in bulk solution. This article describes an investigation into the effects of nanoscale confinement on the crystallization of the inorganic compound potassium ferrocyanide, $\text{K}_4\text{Fe}(\text{CN})_6$ (KFC). Selected for study due to its high solubility, rich polymorphism and interesting physical properties, $\text{K}_4\text{Fe}(\text{CN})_6$ was precipitated within controlled pore glasses (CPG) with pore diameters of 8, 48 and 362 nm. Remarkable effects were seen, such that although anhydrous potassium ferrocyanide was never observed on precipitation in bulk aqueous solution, it was the first phase to crystallize within the CPGs and was present for at least 1 day in all three pore sizes. Slow transformation to the metastable tetragonal polymorph of the trihydrate $\text{K}_4\text{Fe}(\text{CN})_6 \cdot 3\text{H}_2\text{O}$ (KFCT) then occurred, where this polymorph was stable for a month in 8 nm pores. Finally, conversion to the thermodynamically stable monoclinic polymorph of KFCT was observed, where this phase always found after a few minutes in bulk solution. As far as we are aware these retardation effects – by up to five orders of magnitude in the 8 nm pores – are far greater than any seen previously in inorganic systems, and provide strong evidence for the universal effects of confinement on crystallization.

*corresponding author: e-mail h.k.christenson@leeds.ac.uk

† corresponding author: e-mail f.meldrum@leeds.ac.uk

INTRODUCTION

A range of common approaches exist to control crystallization processes in bulk solution, including definition of the solution composition and temperature, and the use of soluble additives.^{1,2} Soluble additives can be particularly effective in defining crystal sizes, morphologies and polymorphs,³ delivering for example, crystalline particles with complex hierarchical structures.⁴⁻⁸ The encapsulation of additives within the crystal lattice can also change the textures,⁹ mechanical properties,¹⁰⁻¹² and optical properties^{13,14} of crystals. As an alternative to additive-directed crystallization, it is also becoming increasingly evident that the micro-environments in which crystals form can themselves define crystallization pathways and products.¹⁵⁻¹⁹ Not only is this of particular importance to processes that naturally occur in confinement such as weathering, biomineralization and the manufacture of nanomaterials, but confinement can potentially provide a stand-alone means of controlling crystallization.

Recent studies by us and others have shown that confinement can have multiple effects on crystallization. A number of studies have focused on organic compounds, where these have shown effects such as the stabilization of amorphous and metastable phases, and preferred orientation.^{18,20,21} Looking then at biologically-relevant solids such as calcium carbonate and calcium sulfate, confined volumes can provide environments that can control the formation of single crystals with complex morphologies.^{7,22-24} Using systems including a crossed-cylinders apparatus,^{19,25,26} arrays of picolitre droplets,²⁷ vesicles that offer confinement in the general range 50 nm – 50 μ m,²⁸⁻³⁰ and the pores of track-etched membranes,³¹⁻³³ it has also been demonstrated that the lifetimes of amorphous precursor phases and metastable crystalline polymorphs of calcium carbonate, calcium phosphate, calcium sulfate and calcium oxalate can be significantly extended, even in micron-scale environments. While this length scale is relevant to many biomineralization processes, crystallization in the environment (eg.

in porous solids) and materials synthesis, there are many crystallization processes which occur in the nanoscale, such as the mineralization of collagen or the formation of nanoparticles.^{31,34,35}

This article describes initial studies of the effects of nanoscale confinement on the precipitation of the inorganic compound potassium ferrocyanide ($K_4Fe(CN)_6$), (potassium hexacyanoferrate (II), KFC), using porous glasses with three different mean pore diameters (8, 48 and 362 nm) as the crystallization environment. Controlled pore glasses (CPGs) are a silica material of a refractory nature containing random and tortuous pores which are available with mean pore diameters from 3 to hundreds of nanometers. They have been frequently used to confine substances like hydrogen and helium, inert gases, water and organic liquids as well as metals for studies of melting and freezing point depression,³⁶ and the properties of confined liquids and solids in general. Recently, CPGs have been used to study the polymorphism of organic crystals such as pimelic acid, glutaric acid and coumarin,²⁰ and certain pharmaceuticals,^{37,38} and in common with the precursor phases of biominerals,^{19,25,26} the metastable phases of organic crystals also increased in stability when confined in 7.5 nm CPGs.^{39,40} $CaCO_3$ has also been precipitated in association with functionalized CPGs,⁴¹ although crystallization occurred both within the CPGs and on their surfaces, making differentiation between the two environments challenging.

Through the use of controlled pore glasses, our study provides a first investigation of the effects of nanoscale confinement on the precipitation of an inorganic solid. Our results show that the smallest pores of the CPGs have extremely strong effects on crystallization such that anhydrous potassium ferrocyanide – which is never observed on precipitation from bulk aqueous solutions – is precipitated as the first phase, and is stable for significant periods of time. A clear pathway of transformation between polymorphs is also observed in the CPGs, providing a clarification of the crystallization mechanism of this material. These results are

of significance to the many crystallization processes that occur within constrained volumes, and the demonstration that the crystallization of inorganic solids can be performed within CPGs opens up new possibilities for performing *in situ* studies of crystallization in confinement.

MATERIALS AND METHODS

Potassium ferrocyanide was precipitated within particles of controlled pore glasses (CPGs) with pore diameters of 362 nm, 48 nm and 8 nm to determine the effect of confinements on the polymorphs generated. These are denoted as CPG-8, CPG-48 and CPG-362 respectively. The results were compared with control experiments performed in bulk solutions.

Materials and General Methods. Potassium ferrocyanide trihydrate (KFCT) was obtained from Sigma-Aldrich, while the controlled pore glasses were obtained from Millipore as particles of diameter 10-100 μm in the case of CPG-48 and CPG-8, and of diameter 1-3 mm in the case of CPG-362. The CPGs were cleaned in 20% nitric acid at 100 °C for 2 h, and were then washed with water followed by ethanol (99% VWR Chemicals), in which they were left overnight before drying under vacuum for 5 h. All glassware including microscope slides for the crystal growth were cleaned overnight in "piranha solution" (30% H_2O_2 and 70% H_2SO_4), then rinsed with Milli-Q water and stored under Milli-Q water until required.

Crystallization in Bulk Solution. Two different methods were used to crystallize KFCT in bulk solution at ambient conditions. Slow crystallization was achieved by allowing 10 mL of concentrated KFCT solution (~20 w/v % - the solubility limit is 29 g/100 ml water) to evaporate in droplets on a glass slide under ambient conditions. Crystals were checked on the glass slides after 3, 5, 10 and 30 min and after complete evaporation of the solution (about 24 h). More rapid crystallization (less than 1 minute) was achieved using ethanol as a precipitant. 50 mL of ethanol were added to 10 mL of KFCT solution (~2 w/v %) and the

crystals were then collected prior to examination using optical microscopy. Unless otherwise stated, ambient conditions are $T = 20 \pm 2$ °C and a relative humidity (r.h.) of 40 ± 5 %.

Crystallization in Controlled Pore Glasses (CPGs). Crystallization in the CPGs was carried out by suspending the porous glass particles in a 20 w/v% solution of KFCT and applying vacuum to remove the gas present within the pores. Sequences of 5-10 mins of pumping were repeated until no more bubbles were observed, and the bulk KFCT solution was then removed by filtration. The particles were then dried by placing them under vacuum for 5 h (rapid drying), or maintaining them under ambient conditions in the laboratory (slow drying). In both cases, crystallization occurs due to evaporation of water from the pores of the CPGs in less than 5 h.

Characterization Methods. The CPG particles were imaged prior and subsequent to crystallization using a FEI Nova NanoSEM 450 scanning electron microscope operating at 1-5 kV. Samples for scanning electron microscopy (SEM) were mounted on SEM stubs using conductive carbon tapes and coated with 2 nm of Ir using a Cressington 208HR high resolution sputter coater. Samples of the crystals precipitated in bulk were investigated with high transmission electron microscopy (TEM) and they were prepared by placing a droplet of the ethanol suspension containing the KFCT crystals on a carbon-covered Cu TEM grid, then analyzed with FEI Tecnai TF20 FEGTEM operating at 200 kV. The presence of crystals in the CPGs was demonstrated by BET surface area analysis using an ASAP 2020 (Accelerated Surface Area and Porosimetry System) with 100 mg of CPG samples analyzed before and after crystallization.

The polymorphs of the crystals precipitated in bulk and within the CPG particles were characterized using a Nikon eclipse LV100 optical microscope (where applicable), Raman microscopy, infrared spectroscopy (IR), powder X-ray diffraction (XRD) and electron diffraction. Raman measurements were carried out at 20-22 °C in the region 2000-2200 cm^{-1} ,

where the CN stretching modes are located, using a Renishaw 2000 Raman microscope with a 785 nm diode laser. The IR analysis was performed using a Perkin Elmer Spectrum 100 FTIR with diamond ATR, and the samples were scanned 5 times at a 4 cm^{-1} spectral resolution. Powder X-ray diffraction was carried out with an X'Pert Phillips XRD diffractometer with spinner configuration. Samples were placed in a sample holder and data were collected at 2θ between 10° and 60° in intervals of 0.033° at a scan rate of $0.119^\circ\text{ min}^{-1}$. Electron diffraction of the crystals in bulk was recorded using selected-area electron diffraction (SAED) using 1 μm aperture. Electron diffraction and PXRD diffraction of the crystals were simulated using CrystalMarker software.

RESULTS

Potassium ferrocyanide was selected as the focus of this study due to its high solubility (which facilitates significant pore-filling and removal of surface crystals from the CPGs) and its rich polymorphism; it crystallizes at room temperature as an anhydrous form (KFC), and as hydrated polymorphs of potassium ferrocyanide trihydrate (KFCT), as summarized in Table 1. KFCT has a metastable tetragonal form and a thermodynamically stable monoclinic polymorph, and also exhibits a number of twinned crystals.^{42,43} Potassium ferrocyanide is used in the food industry to prevent the caking of table salt and to precipitate heavy metals from wine,⁴⁴ and has applications as a catalyst, an ion exchanger, photosensitizer and a supramolecular magnetic material.^{45,46} KFCT also exhibits a number of unusual solid-state transitions, which have elicited considerable interest from a fundamental point of view.⁴⁷⁻⁴⁹

Crystallization in Bulk Solution. Two precipitation methods were employed; evaporation of aqueous solutions or precipitation from aqueous solution by ethanol addition. When potassium ferrocyanide solutions (2-20 w/v %) were allowed to evaporate under ambient ($T = 20\text{-}22\text{ }^\circ\text{C}$, relative humidity $35\pm 5\%$) conditions two types of crystals with distinct

morphologies precipitated. The first crystals formed after 3 min were hexagonal in shape (Figure 1a), while a mixture of hexagonal-shaped and rectangular prismatic crystals was observed after 10 min (Figure 1b). The proportion of rectangular crystals increased with time (although a mixture of both crystal shapes was typically found), where these were stable at room temperature and grew to millimeter sizes upon complete evaporation.

As an alternative precipitation method, 50 mL of ethanol was added to 10 mL dilute (2 w/v%) solutions of KFCT, which resulted in immediate formation of white, needle-shaped crystals (Figure 1c). These crystals were unstable in solution and redissolved within 5 min, being replaced with crystals that grew into irregular, octagonal prisms (Figure 1d). These subsequently either transformed directly into rectangular prisms or dissolved and then reprecipitated as the rectangular prisms or hexagons seen on evaporation of aqueous solutions over \approx 10 min. Figure 2 shows a sequence of images that illustrates the morphological evolution of crystals formed by ethanol precipitation. This progression in crystal morphologies is consistent with descriptions of crystals of KFCT in the literature, which assigns the rectangular prismatic crystals to the monoclinic polymorph.⁵⁰

The crystal structures of the different morphological forms of KFCT were then investigated using Raman microscopy and infrared spectroscopy (IR), powder X-ray diffraction (PXRD) and TEM selective area electron diffraction (SAED) to determine their polymorphs, where the assignments are summarized in Table 1. Samples for IR and PXRD analyses were recovered by filtration, where this was carried out 1 min after initiation of the reaction in the ethanol precipitation, and after 3 min from the evaporating solutions. The samples obtained from ethanol precipitation principally comprised needle-shaped crystals, together with minor amounts of hexagonal and rectangular crystals, while those from the evaporating solutions were principally hexagonal crystals, together with some rectangular crystals. The proportion of rectangular crystals could be increased by isolating the crystals after longer reaction times.

As the samples for IR and PXRD invariably comprised mixtures of the two polymorphs, these techniques could not be used to assign polymorph to a precise crystal morphology. Crystals precipitated by evaporation exhibited the same IR spectra at long or short reaction times (Figure 3a), where the bands at 3587, 3518, 3375, 1647 and 1614 cm^{-1} derive from O-H bond stretching of the water molecules, and the band at 2035 cm^{-1} derives from the symmetric stretching of the CN-group.⁵⁰ The IR spectrum of the ethanol-precipitated samples containing needle-shaped crystals was distinctly different (Figure 3b). The major OH-bands in a range 3300- 3600 cm^{-1} were very weak, the 1614 cm^{-1} OH bands were significantly reduced in intensity and new peaks in the CN-region at 2093, 2072, 2017 and 2041 cm^{-1} were observed. These data demonstrate that the needle-shaped crystals correspond to the anhydrous phase (potassium ferrocyanide, KFC), where this was confirmed by PXRD. Ethanol-precipitated samples, where needle-shaped crystals were present, gave powder diffraction peaks corresponding to anhydrous KFC and KFCT (Figure 4a). That the peaks are more intense for KFCT can be attributed to the fact that although there are fewer crystals, they are larger in size and similarly oriented due to their plate-like shape. PXRD analysis of the samples isolated from the evaporation reactions after 3 min demonstrated that the crystals were hydrated KFCT (monoclinic or tetragonal) (Figure 4b); no peaks corresponding to KFC were observed. Analysis of samples prepared at longer times yielded very similar diffraction patterns (Fig S1). It is noted that the PXRD spectra of the tetragonal and monoclinic polymorphs are very similar, making it very difficult to determine the proportions of each of these forms in a mixed powder as shown in simulated patterns (Figure S2)

Raman analysis was performed of individual crystals, and showed that all of the morphological forms have a main peak at 2090 - 2093 cm^{-1} . The rectangular and octagonal crystals showed Raman peaks at 2064 cm^{-1} and 2093 cm^{-1} (Figures 5a and 5b), where these

correspond to the ν_1 and ν_3 bands of monoclinic KFCT crystals.⁵⁰ These data therefore suggest the rectangular and octagonal crystals have identical structures, and are simply different morphological forms of the monoclinic polymorph. This is also supported by *in situ* observation of their crystallization by optical microscopy, which revealed that the diagonal edge of the octagonal crystals often grew faster than the other edges, transforming the shape into a rectangular one (Figure 2). The hexagonal crystals showed two additional peaks at approximately 2023 cm^{-1} and 2039 cm^{-1} , and the peak at 2064 cm^{-1} appeared to have split into two, at 2023 cm^{-1} and 2039 cm^{-1} (Figures 5c), as is consistent with the reported Raman spectrum of the hexagonal crystals.⁵¹ The Raman spectrum of the ethanol-precipitated needle-shaped crystals was very similar to that of the tetragonal form (Figure 5d), but measurements on the anhydrous phase obtained by heating the supplied bulk KFCT confirmed this similarity (Figure 5e).

Selected-area electron diffraction (SAED) was used to provide further confirmation of the polymorph assignments, where this can again be used to analyze individual crystals. A summary of the diffraction pattern assignments and comparison with the monoclinic and tetragonal crystal systems is provided in the supplementary information (text and Table S1 and Figure S3). The SAED data demonstrated that the rectangular and octagonal crystals both correspond to the monoclinic form of KFCT⁴² (Figures 6a, 6b and 6c and 6d), while the hexagonal-shaped crystals are tetragonal (Figure 6e and 6f).⁵²

Effects of Humidity on Crystals Precipitated in Bulk. The stabilities of the different crystal polymorphs in humid air ($\approx 100\%$ humidity) were investigated due to their relevance to the long-term incubation of the CPG/KFC particles in air. Under these conditions, the hexagonal-shaped crystals of the tetragonal polymorph transformed to the monoclinic polymorph (rectangular crystals) in 15 mins, as shown by optical microscopy and Raman spectroscopy. The effects of humidity on the orthorhombic KFC phase (needle-shaped

crystals) obtained by ethanol precipitation were also studied at close to 100 % humidity. KFC redissolved in under 5 min as observed by optical microscopy after which time a mixture of monoclinic and tetragonal KFCT crystals precipitated. After a further 15 min only the stable monoclinic polymorph was evident (Figure S4). Notably, neither the anhydrous KFC nor the tetragonal polymorph converted into the monoclinic form under ambient conditions (of humidity 40 ± 5 %) over a time span of 1 month.

Crystallization in Controlled Pore Glasses (CPGs). Crystallization of KFC within the CPGs was achieved by infiltrating the CPGs with a solution of KFC, filtering off the bulk solution, and then allowing the CPG particles to either dry slowly in air under laboratory conditions, or rapidly under vacuum. This procedure ensured that bulk KFCT crystals did not precipitate on the surfaces of the CPGs, or between particles of CPGs, where this was confirmed using scanning electron microscopy (SEM) (Figure S5). BET analysis showed a marked decrease of surface area in CPG-48 and CPG-8 after crystallization (Table S2), whereas the decrease with CPG-362 was insignificant. Although the results are only qualitative, they do suggest a considerable incorporation of crystals in to the CPGs, at least for the two smaller pore sizes.

The crystals formed inside the CPG particles were studied at different times using PXRD, Raman and IR spectroscopy. Markedly different results were obtained compared to the bulk crystallization experiments, where a summary is presented in Table 2. In all of the pores sizes, and under all experimental conditions, crystals of the anhydrous KFC invariably precipitated first, as confirmed by PXRD. Within vacuum-dried CPGs, the KFC crystals remained unchanged for after 1 month in ambient conditions (Figure S6) and conversion to KFCT with time was not observed (for at least 1 year). By contrast, air-dried CPGs samples of all pore sizes showed differences in polymorph conversion with time. After initial formation of KFC crystals, the hydrated KFCT crystals began to appear with time, which was

confirmed by IR (Figure S7), XRD (Figures 7, 8 and 9) and Raman (Figure S8). KFC persisted in the CPG-362 and the CPG-48 for one day, while it was still found after a month in the CPG-8 according to PXRD analysis (Figure 9). Note that the background intensity from the glass varies considerably between samples, and that the CPG-362 particles are much bigger than the other two, which makes any quantification based on relative peak heights or areas difficult.

After complete transformation from anhydrous KFC to tetragonal or monoclinic KFCT, as confirmed by XRD, Raman analysis was carried out to estimate the proportions of the monoclinic and tetragonal forms in the CPGs. After two days, Raman spectra of at least 20 particles of the three different CPGs were recorded, showing that the KFCT crystals in CPG-362 and CPG-48 consisted of $\approx 70\%$ of the monoclinic polymorph and 30% of the tetragonal form (Figure S9). Particles with peaks overlapping were not included in the percentages. In contrast, in CPG-8, only the tetragonal polymorph was present for up to one month. Incubation times over a month eventually led to further transformation, and the presence of a mixture of the monoclinic and tetragonal polymorphs in all three pore sizes. It was also noted that the CPG vacuum-dried particles remained white for one year, while the air-dried samples turned from white to yellow with time, reflecting the color change undergone by the anhydrous KFC as it transforms into KFCT crystals.

Effect of Humidity on the Transformation of Crystals in CPGs. The influence of humidity on crystal transformation was studied by storing the CPG/KFC samples at 100 % humidity and monitoring them using IR analysis. Anhydrous KFC crystals in vacuum-dried CPGs took 2 days before fully transforming to a mixture of KFCT phases within the CPG-48 and CPG-362 (Figure S10), while in the CPG-8 the IR absorption bands corresponding to KFCT only became apparent after 2 weeks (Figure S11). In the air-dried CPG-8 the tetragonal KFCT crystals remained stable for up to 1 h before transforming to monoclinic

crystals under humid conditions (Figure S12). For comparison, this process took 15 min under same conditions in bulk. These observations are summarized in Figure 10.

DISCUSSION

Our results describing the precipitation of KFC in bulk are in good agreement with the literature. In 1869, Wyrouboff managed to identify likely monoclinic and tetragonal polymorphs by light microscopy alone,⁵³ while in 1911 Briggs presented micrographs of crystals with rectangular, hexagonal and octagonal prismatic habits.^{54,55} More recent studies have revealed the complexity of the KFCT system, and have shown that it comprises a number of polymorphs which are very close in free energy.^{42,43,47,49,51} The five different forms include a monoclinic and a tetragonal polymorph and three different twinned crystals. The stable monoclinic crystals of KFCT have been isolated and characterized by a range of techniques,⁵⁰ but to the best of our knowledge, no Raman or IR data of tetragonal KFCT have been reported in the literature. A mixture of these two polymorphs is also typically precipitated in bulk solution, which has limited the characterization of the tetragonal polymorph.⁴²

The experiments carried out in this study have shown the existence of four crystal-types with clearly distinguishable morphologies (irregular, octagonal, rectangular and hexagonal) on crystallization of KFCT from aqueous solution at room temperature. The needle-shaped crystals observed on ethanol precipitation correspond to anhydrous KFC, whereas if anhydrous KFC forms on evaporation of aqueous solution it is too short-lived to be detected visually. The rectangular form corresponds to the monoclinic polymorph of KFCT,⁵⁰ while our observations that the octagonal crystals exhibit identical Raman and IR spectra and electron diffraction patterns to their rectangular counterparts suggest that they are just an early stage of growth of the monoclinic polymorph. Finally, the crystals with hexagonal

shape that are observed at short crystallization times, are shown to be tetragonal KFCT by Raman and electron diffraction data.

Markedly different results were obtained on precipitation of KFC in confinement. That crystallization proceeds more slowly in the CPG pores enabled the transformation pathway to be more clearly resolved, and a more orderly progression from anhydrous crystal to tetragonal trihydrate to monoclinic trihydrate was observed. As highlighted above, a mixture of the tetragonal and monoclinic polymorphs (including twinned forms) are invariably present in bulk solution, from the moment that crystals first appear until at least six months later. In stark contrast, anhydrous KFC was the first phase formed in confinement under all experimental conditions, and was never observed on precipitation of KFC from bulk aqueous solution. This cannot be due to a lack of available water – at the solubility limit there are 68 moles of water available for every mole of $K_4Fe(CN)_6$, or more than 20 times the amount needed to form the hydrated salt. An effect of confinement on the nucleation of the trihydrate also appears unlikely, as even the smallest pore diameter of 8 nm is likely to be much larger than the size of a critical nucleus for any reasonable supersaturation.

Having formed, the anhydrous KFC crystals can be stable for long periods in the CPGs. On drying the CPGs rapidly (under vacuum) anhydrous KFC was stable for at least 1 year in all pore sizes, as compared with a few days for air-dried samples. It is likely that drying under vacuum removes all water from the porous glass, and that the complete absence of water is responsible for the long-term stability of KFC in the pores, since the ambient humidity diffusing in from the environment is insufficient to convert the anhydrous salt to the trihydrate. A similar effect has been observed with β -glycine stabilized in the nanopores of anodic aluminum oxide (AAO).⁵⁶ By contrast, when the porous glass is dried under ambient conditions, enough water must be left in the pores to be able to slowly hydrate the anhydrous crystals over days to months. This comparatively slow rate of hydration must be due at least

partly to a reduced rate of diffusion of water, whether liquid or in the form of vapor, through the pores. In addition to the reduced diffusion rate there must also be a blocking effect of existing crystals in the pores, as they will cut off many available pathways of diffusion. Finally, as our observations of the transformation of the bulk crystals between polymorphs suggests that hydration occurs by a dissolution/ reprecipitation mechanism, the process will also depend on the requirement for nucleation events in what may be a very limited volume of solution.

A much slower transformation from the metastable tetragonal polymorph to the stable monoclinic form was also observed in the CPGs as compared with bulk solution. While the water contents of the tetragonal and monoclinic polymorphs are the same, it is known that the presence of water is necessary for the transformation in bulk. Finally, the lifetime of the metastable tetragonal polymorph was greatest in the smallest pores, showing that this polymorph is more stable in small volumes than in larger pores or bulk, where conversion to the monoclinic polymorph was more rapid.

Our samples are such that the mean pore diameter may be considered large as compared to the diameters of the diffusing species; water, potassium ions and ferrocyanide ions.⁵⁷ Experimentally, a hindrance factor, or reduction in the diffusion coefficient, of some 5 times has been found for water diffusing in sol-gel glass of mean pore diameter 3.5 nm. As another example, the effective diffusion coefficient for cyclohexane was found to vary between 0.37 and 0.91 of the bulk value for pore diameters of 6 to 49 nm.⁵⁸ Since the time t taken to diffuse a certain distance is inversely proportional to the diffusion coefficient D , it follows that the effect of confinement on the diffusion rate even in the smallest pores is at most a factor of 5, and would be hardly noticeable in the largest pores. There are other effects which might act to slow down the diffusion further, such as adsorption to the pore walls, electrostatic interactions between the ions and the silica surfaces, and the tortuosity of the

pores,⁵⁹ but these are again unlikely to be significant in the pore sizes employed here. Hindered diffusion is hence very unlikely to be the major factor in the confinement effects seen. Alternative possibilities include a decrease in convective transport of material, which has been shown to dominate over diffusive transport in bulk crystal growth,⁶⁰ and the likely requirement for a large number of nucleation events to convert a significant fraction of highly dispersed metastable phase to a more stable polymorph.

The much longer time taken for the stable monoclinic polymorph to appear in the smallest pores is consistent with other studies of crystallization in confinement, which have also shown that metastable phases are stabilized in confined volumes.^{19,25,28,61} Focusing in particular on inorganic solids, the crossed cylinder apparatus has been particularly valuable in studying crystals formed between surfaces separated by distances as small as ≈ 200 nm. Crystallization through a sequence of metastable polymorphs was observed in the calcium carbonate,²⁵ calcium phosphate¹⁹ and calcium sulfate systems,²⁶ where factors such as the difficulty of dehydration of hydrated amorphous calcium carbonate particles,²⁵ and the hindered aggregation of precursor particles of calcium sulfate²⁶ between two closely apposed surfaces may have contributed to these effects. However, that significant confinement effects have been observed in every inorganic crystal system that we have examined suggests that this phenomenon has a common underlying physical mechanism. Further, that these effects can operate even on the micron-scale shows that this does not originate from the pore-size dependent stabilization of critical nuclei, as is often suggested for organic compounds^{39,40,62}. Our demonstration that it is possible to crystallize inorganic crystals within controlled pore glasses now opens the door to *in situ* studies of crystallization in constrained volumes, where these are expected to provide new understanding of these confinement effects.

CONCLUSIONS

This study has demonstrated that controlled pore glasses (CPGs) can be used as an effective means of studying the effects of nanoscale confinement on the crystallization of inorganic compounds. Focusing on the precipitation of potassium ferrocyanide $K_4Fe(CN)_6$ from aqueous solution within CPGs with pore diameters of 8, 48 and 362 nm, we observed a different crystallization pathway to that seen in bulk solution. The first phase to crystallize within the CPGs was the anhydrous salt of potassium ferrocyanide (KFC), which was not observed when precipitating by evaporation of a bulk aqueous solution. The KFC confined to the pores transforms slowly over days to the trihydrate (KFCT) in the presence of water in the pores, whereas the conversion in a humid environment in bulk takes less than 5 min. The metastable tetragonal polymorph of KFCT persists for only 15 minutes in humid conditions or as a mixture with the monoclinic polymorph at ambient conditions whereas it is possible to detect it in 8 nm pores for a month. In the smallest pores the thermodynamically stable monoclinic polymorph of KFCT only appears after 2 months, compared to the minutes it takes in bulk solution. The effect of confinement is hence to slow down significantly – by 4 to 5 orders of magnitude in the 8 nm pores – the sequential crystallization of polymorphs of potassium ferrocyanide. This strongly suggests that this is a universal effect of confinement on crystallization, regardless of details of the structure and nature of the polymorphs involved. Once again it has been shown that crystallization in confinement is a useful means of observing polymorphs that have only transient existence in bulk solution.

ASSOCIATED CONTENT

Supporting Information. The Supporting Information is available free of charge on the ACS Publications website at DOI: <http://doi.org/10.5518/76>

Data Availability: The supporting information, optical microscopy, PXRD, Raman, IR, SEM and TEM raw data that support the findings of this study are available in the “Research Data Leeds Repository” with the identifier <http://doi.org/10.5518/76>⁶³

AUTHOR INFORMATION

Corresponding Authors * (H.K.C.) E-mail: h.k.christenson@leeds.ac.uk † (F.C.M.) E-mail: F.meldrum@leeds.ac.uk.

Notes The authors declare no competing financial interest.

ACKNOWLEDGMENTS

This work was supported by a UK Engineering and Physical Sciences (EPSRC) Leadership Fellowship (FCM, EP/H005374/1) and an EPSRC Platform Grant (FCM and HKC, EP/N002423/1).

Morphology	Assignment	Crystal System	Crystallographic parameters	
Needle-like crystals	Anhydrous KFC	Orthorhombic Cmc _m	Alpha = beta = gamma = 90 °	a (Å): 4.18 b (Å): 14.01 c (Å): 21.04
Rectangular prism	KFCT	Monoclinic C2/c	Alpha = gamma = 90 ° Beta = 90.69-90.096 °	a (Å): 9.38-9.40 b (Å): 16.84-16.88 c (Å): 9.39-9.41
Octagonal prism	KFCT	Monoclinic C2/c	Alpha = gamma = 90 ° Beta = 90.69-90.096 °	a (Å): 9.38-9.40 b (Å): 16.84-16.88 c (Å): 9.39-9.41
Hexagonal crystal	KFCT	Tetragonal I41/a	Alpha = beta = gamma = 90 °	a (Å): 9.39-9.41 b (Å): 9.39- 0.41 c (Å): 33.67-33.72

Table 1. Summary of the crystals precipitated from bulk solutions of potassium ferrocyanide, where KFC corresponds to the anhydrous form, $K_4Fe(CN)_6$, and KFCT to the trihydrate. Needle-like crystals (yellow) are assigned to orthorhombic KFC, rectangular and octagonal prisms (turquoise) are the monoclinic polymorph of KFCT and hexagonal-shaped crystals (pink) are the tetragonal polymorph of KFCT.^{42,49,52,64}

Air-dried					Vacuum-dried
Incubating time	Bulk solution	CPG-362 nm	CPG-48 nm	CPG- 8nm	CPG-362, CPG-48, CPG-8
<i>1 h to 1 day</i>	KFCT (polymorph mixture)	KFC	KFC	KFC	KFC
<i>2 days</i>	KFCT (polymorph mixture)	KFC + KFCT (polymorph mixture)	KFC + KFCT (polymorph mixture)	KFC + tetragonal KFCT crystals	KFC
<i>3 days to 1 month</i>	KFCT (polymorph mixture)	KFCT (polymorph mixture)	KFCT (polymorph mixture)	KFC + tetragonal KFCT crystals	KFC
<i>>1 month</i>	KFCT (polymorph mixture)	KFCT (polymorph mixture)	KFCT (polymorph mixture)	KFCT (polymorph mixture)	KFC

Table 2. Summary of data obtained on precipitating a KFC within CPG particles of the indicated pore sizes, and then drying the CPG/KFC particles in air or under vacuum. The yellow color corresponds to orthorhombic KFC, the turquoise to monoclinic KFCT and pink to tetragonal KFCT. The anhydrous KFC precipitated first in the CPGs and transformed into KFCT with time. After a month, a mixture of polymorphs (typically ca. 70% monoclinic and ca. 30% of the tetragonal) was found in all three pore sizes. In the vacuum-dried pores the initially precipitated KFC remained stable for at least 1 year. The table also provides a comparison with crystals precipitated on evaporation of a bulk solution, where a mixture of KFCT polymorphs is always observed and the proportion of monoclinic crystals increased with time.

REFERENCES

- (1) Wu, Z. H.; Yang, S. L.; Wu, W., *Nanoscale* **2016**, 8, 1237-1259.
- (2) Song, R. Q.; Colfen, H., *CrystEngComm* **2011**, 13, 1249-1276.
- (3) Meldrum, F. C.; Coelfen, H., *Chem. Rev.* **2008**, 108, 4332-4432.
- (4) Schenk, A. S.; Zlotnikov, I.; Pokroy, B.; Gierlinger, N.; Masic, A.; Zaslansky, P.; Fitch, A. N.; Paris, O.; Metzger, T. H.; Colfen, H.; Fratzl, P.; Aichmayer, B., *Adv. Funct. Mater.* **2012**, 22, 4668-4676.
- (5) Zhou, Y. L.; Marson, R. L.; van Anders, G.; Zhu, J.; Ma, G. X.; Ercius, P.; Sun, K.; Yeom, B.; Glotzer, S. C.; Kotov, N. A., *ACS Nano* **2016**, 10, 3248-3256.
- (6) Gower, L. B.; Odom, D. J., *J. Cryst. Growth* **2000**, 210, 719-734.
- (7) Yue, W. B.; Park, R. J.; Kulak, A. N.; Meldrum, F. C., *J. Cryst. Growth* **2006**, 294, 69-77.
- (8) Cantaert, B.; Kim, Y. Y.; Ludwig, H.; Nudelman, F.; Sommerdijk, N.; Meldrum, F. C., *Adv. Funct. Mater.* **2012**, 22, 907-915.
- (9) Borukhin, S.; Bloch, L.; Radlauer, T.; Hill, A. H.; Fitch, A. N.; Pokroy, B., *Adv. Funct. Mater.* **2012**, 22, 4216-4224.
- (10) Kim, Y. Y.; Carloni, J. D.; Demarchi, B.; Sparks, D.; Reid, D. G.; Kunitake, M. E.; Tang, C. C.; Duer, M. J.; Freeman, C. L.; Pokroy, B.; Penkman, K.; Harding, J. H.; Estroff, L. A.; Baker, S. P.; Meldrum, F. C., *Nat. Mater.* **2016**, 15, 903-10.
- (11) Kim, Y. Y.; Ribeiro, L.; Maillot, F.; Ward, O.; Eichhorn, S. J.; Meldrum, F. C., *Adv. Mater.* **2010**, 22, 2082-+.
- (12) Kim, Y. Y.; Ganesan, K.; Yang, P. C.; Kulak, A. N.; Borukhin, S.; Pechook, S.; Ribeiro, L.; Kroger, R.; Eichhorn, S. J.; Armes, S. P.; Pokroy, B.; Meldrum, F. C., *Nat. Mater.* **2011**, 10, 890-896.
- (13) Brif, A.; Ankonina, G.; Drathen, C.; Pokroy, B., *Adv. Funct. Mater.* **2014**, 26, 477-481.
- (14) Kulak, A. N.; Yang, P. C.; Kim, Y. Y.; Armes, S. P.; Meldrum, F. C., *Chem. Comm.* **2014**, 50, 67-69.
- (15) Gong, X. Q.; Wang, Y. W.; Ihli, J.; Kim, Y. Y.; Li, S. B.; Walshaw, R.; Chen, L.; Meldrum, F. C., *Adv. Mater.* **2015**, 27, 7395-+.
- (16) Falini, G.; Fermani, S.; Gazzano, M.; Ripamonti, A., *Chem. Eur. J.* **1998**, 4, 1048-1052.
- (17) Falini, G.; Albeck, S.; Weiner, S.; Addadi, L., *Science* **1996**, 271, 67-69.
- (18) Jiang, Q.; Ward, M. D., *Chem. Soc. Rev.* **2014**, 43, 2066-2079.
- (19) Wang, Y.-W.; Christenson, H. K.; Meldrum, F. C., *Chem. Mat.* **2014**, 26, 5830-5838.
- (20) Ha, J.-M.; Hamilton, B. D.; Hillmyer, M. A.; Ward, M. D., *Cryst. Growth Des.* **2009**, 9, 4766-4777.
- (21) Nartowski, K. P.; Tedder, J.; Braun, D. E.; Fabian, L.; Khimyak, Y. Z., *Phys. Chem. Chem. Phys.* **2015**, 17, 24761-24773.
- (22) Park, R. J.; Meldrum, F. C., *Adv. Mater.* **2002**, 14, 1167-1169.
- (23) Yue, W. B.; Kulak, A. N.; Meldrum, F. C., *J. Mater. Chem.* **2006**, 16, 408-416.
- (24) Lose, E.; Meldrum, F. C., *Chem. Comm.* **2001**, 901-902.

- (25) Stephens, C. J.; Ladden, S. F.; Meldrum, F. C.; Christenson, H. K., *Adv. Funct. Mater.* **2010**, *20*, 2108-2115.
- (26) Wang, Y.-W.; Christenson, H. K.; Meldrum, F. C., *Adv. Funct. Mater.* **2013**, *23*, 5615-5623.
- (27) Stephens, C. J.; Kim, Y.-Y.; Evans, S. D.; Meldrum, F. C.; Christenson, H. K., *J. Am. Chem. Soc.* **2011**, *133*, 5210-5213.
- (28) Tester, C. C.; Brock, R. E.; Wu, C.-H.; Krejci, M. R.; Weigand, S.; Joester, D., *CrystEngComm* **2011**, *13*, 3975-3978.
- (29) Tester, C. C.; Whittaker, M. L.; Joester, D., *Chem. Comm.* **2014**, *50*, 5619-5622.
- (30) Cacace, D. N.; Rowland, A. T.; Stapleton, J. J.; Dewey, D. C.; Keating, C. D., *Langmuir* **2015**, *31*, 11329-11338.
- (31) Cantaert, B.; Beniash, E.; Meldrum, F. C., *Chem. Eur. J.* **2013**, *19*, 14918-14924.
- (32) Schenk, A. S.; Albarracin, E. J.; Kim, Y. Y.; Ihli, J.; Meldrum, F. C., *Chem. Comm.* **2014**, *50*, 4729-4732.
- (33) Ihli, J.; Wang, Y. W.; Cantaert, B.; Kim, Y. Y.; Green, D. C.; Bomans, P. H. H.; Sommerdijk, N.; Meldrum, F. C., *Chem. Mater.* **2015**, *27*, 3999-4007.
- (34) Nudelman, F.; Pieterse, K.; George, A.; Bomans, P. H. H.; Friedrich, H.; Brylka, L. J.; Hilbers, P. A. J.; de With, G.; Sommerdijk, N. A. J. M., *Nat. Mater.* **2010**, *9*, 1004-1009.
- (35) Meldrum, F. C.; Heywood, B. R.; Mann, S., *Science* **1992**, *257*, 522-523.
- (36) Christenson, H. K., *J. Phys.: Condens. Matter* **2001**, *13*, R95-R133.
- (37) Rengarajan, G. T.; Enke, D.; Steinhart, M.; Beiner, M., *J. Mater. Chem.* **2008**, *18*, 2537-2539.
- (38) Dwyer, L.; Michaelis, V.; O'Mahony, M.; Griffin, R.; Myerson, A., *CrystEngComm* **2015**, *17*, 7922-7929.
- (39) Hamilton, B. D.; Hillmyer, M. A.; Ward, M. D., *Cryst. Growth. Des.* **2008**, *8*, 3368-3375.
- (40) Ha, J. M.; Wolf, J. H.; Hillmyer, M. A.; Ward, M. D., *J. Am. Chem. Soc.* **2004**, *126*, 3382-3383.
- (41) Stack, A. G.; Fernandez-Martinez, A.; Allard, L. F.; Banuelos, J. L.; Rother, G.; Anovitz, L. M.; Cole, D. R.; Waychunas, G. A., *Environ. Sci. Technol.* **2014**, *48*, 6177-6183.
- (42) Willans, M. J.; Wasylishen, R. E.; McDonald, R., *Inorg. Chem.* **2009**, *48*, 4342-4353.
- (43) Gaffar, M. A.; Omar, M. H., *J. Therm. Anal. Calorim.* **2005**, *81*, 477-487.
- (44) Gail, E.; Gos, S.; Kulzer, R.; Lorösch, J.; Rubo, A.; Sauer, M.; Kellens, R.; Reddy, J.; Steier, N.; Hasenpusch, W., Cyano Compounds, Inorganic. In *Ullmann's Encyclopedia of Industrial Chemistry*, Wiley-VCH Verlag GmbH & Co. KGaA: 2000.
- (45) Bernhardt, P. V.; Bozoglian, F.; Macpherson, B. P.; Martínez, M., *Coord. Chem. Rev.* **2005**, *249*, 1902-1916.
- (46) Lescouëzec, R.; Toma, L. M.; Vaissermann, J.; Verdaguer, M.; Delgado, F. S.; Ruiz-Pérez, C.; Lloret, F.; Julve, M., *Coord. Chem. Rev.* **2005**, *249*, 2691-2729.
- (47) Kiriya, R.; Niizeki, N.; Hirabayashi, H.; Wada, T.; Kiriya, H., *J. Phys. Soc. Jpn.* **1964**, *19*, 540-&.

- (48) Blinc, R.; Waugh, J. S.; Brenman, M., *J. Chem. Phys.* **1961**, 35, 1770-&.
- (49) Toyoda, H.; Niizeki, N.; Waku, S., *J. Phys. Soc. Japan* **1960**, 15, 1831-1841.
- (50) Kanagadurai, R.; Sankar, R.; Sivanesan, G.; Srinivasan, S.; Jayavel, R., *Crys. Res. Technol.* **2006**, 41, 853-858.
- (51) Geneviciute, L.; Florio, N.; Lee, S., *Cryst. Growth Des.* **2011**, 11, 4440-4448.
- (52) Povarennykh, A.; Rusakova, L., *Geol. Zh.* **1973**, 33, 245.
- (53) Wyrouboff, *Ann. Chim. Phys.* **1869**, 293-301.
- (54) Briggs, S. H. C., *J. Chem. Soc.* **1911**, 99, 1019-1035.
- (55) Briggs, S. H. C., *J. Chem. Soc.* **1920**, 1026-1034.
- (56) Jiang, Q.; Hu, C.; Ward, M. D., *J. Am. Chem. Soc.* **2013**, 135, 2144-2147.
- (57) Messenger, R.; Chatenay, D.; Urbach, W.; Bouchaud, J. P.; Langevin, D., *Europhys. Lett.* **1989**, 10, 61-66.
- (58) Mitzithras, A.; Coveney, F. M.; Strange, J. H., *J. Mol. Liq.* **1992**, 54, 273-281.
- (59) Shen, L.; Chen, Z., *Chem. Eng. Sci.* **2007**, 62, 3748-3755.
- (60) Kile, D. E.; Eberl, D. D., *Am. Mineral.* **2003**, 88, 1514-1521.
- (61) Lee, S.; Feldman, J.; Lee, S. S., *Cryst. Growth Des.* **2016**, DOI: 10.1021/acs.cgd.6b00801.
- (62) Ha, J.-M.; Hamilton, B. D.; Hillmyer, M. A.; Ward, M. D., *Cryst. Growth Des.* **2012**, 12, 4494-4504.
- (63) Anduix-Canto, C.; Wang, Y.-W.; Kim, Y.-Y.; Kulak, A. N.; Meldrum, F. C.; Christenson, H. K., *Research Data Leeds Repository* **2016**, <http://doi.org/10.5518/76>.
- (64) Standard x-ray diffraction powder patterns. In Natl. Bur. Stand. (U.S): 1981; Vol. 25, p 56.

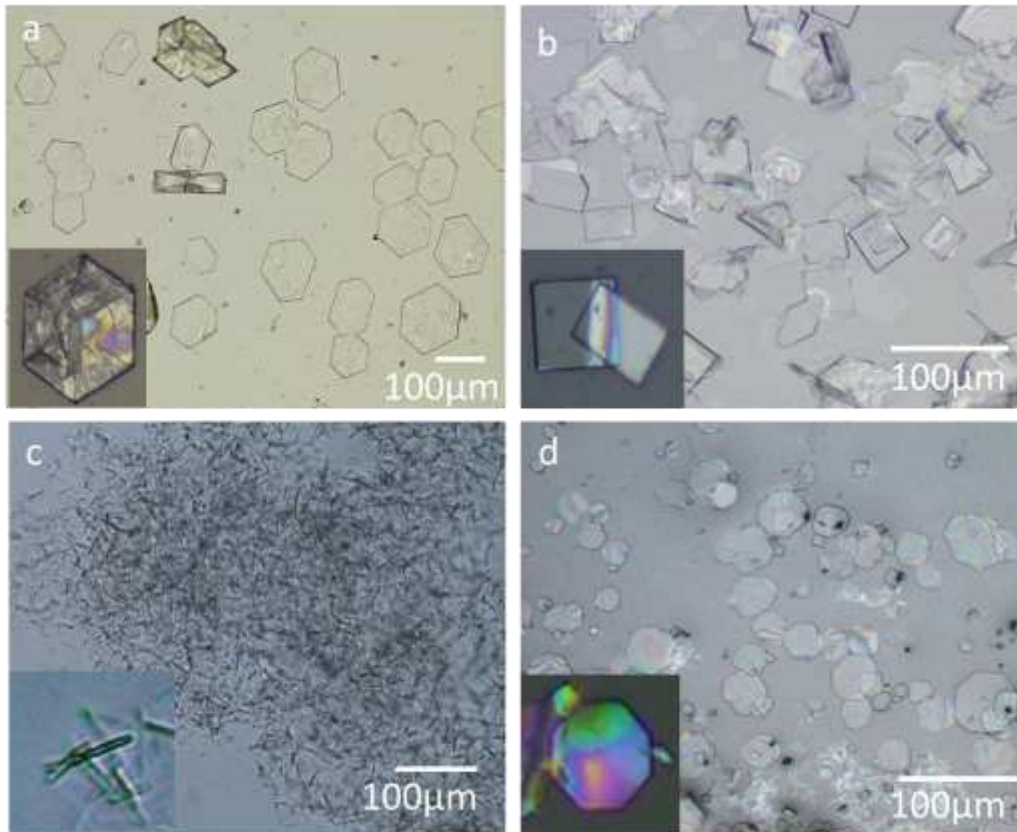


Figure 1. Optical micrographs of KFCT crystals precipitated on evaporation of aqueous solutions of KFCT (a-b) and by ethanol precipitation of KFCT (c-d). (a) Hexagonal crystals observed within 3 min in KFCT solution, (b) after 10 min, rectangular crystals appeared, (c) immediate formation of needle-shaped crystals within 1 min (d) octagonal crystals formed after dissolution of the needle-like crystals.

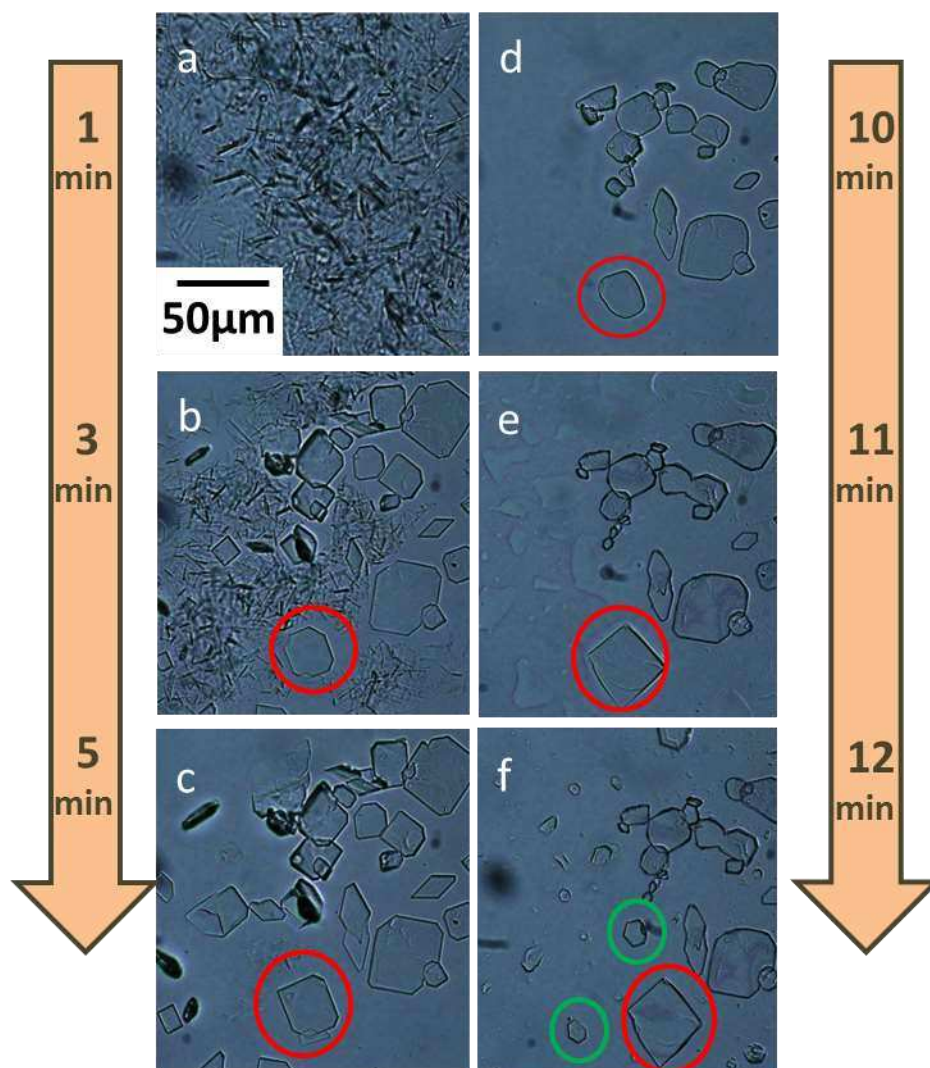


Figure 2. Typical optical microscopy images recorded during the transformation of KFCT crystals obtained by ethanol precipitation after, (a) 1 minute, when only needle-shaped crystals are observed, (b) 3 min, when the needles start to dissolve and are replaced by prismatic crystals with different shapes (an octagonal crystal is circled in red), (c) 5 min, when the needles have dissolved and the octagonal crystal in (b) has become more rectangular, (d) 10 min, when most crystals appear to be dissolving, (e) 11 min, when the octagonal crystal in (b) has transformed into a stable rectangular crystal, and (f) 12 min, when further new crystals have appeared (in green).

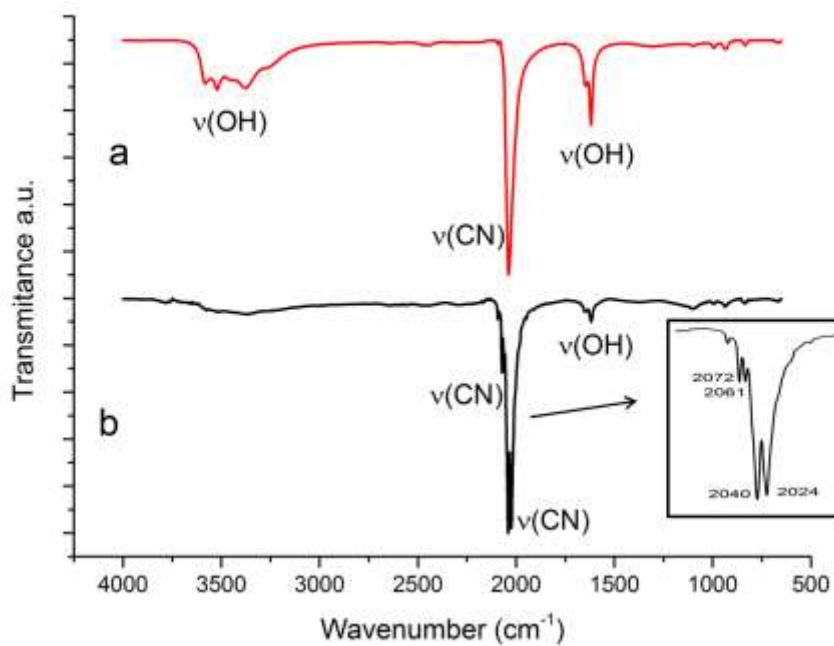


Figure 3. IR spectra of KFCT and KFC crystals, (a) precipitated by evaporation and isolated after short reaction times such that the sample was principally hexagonal-shaped crystals, (b) isolated after 1 min after ethanol precipitation, where the sample principally contains needle-like crystals, together with some hexagonal and rectangular crystals.

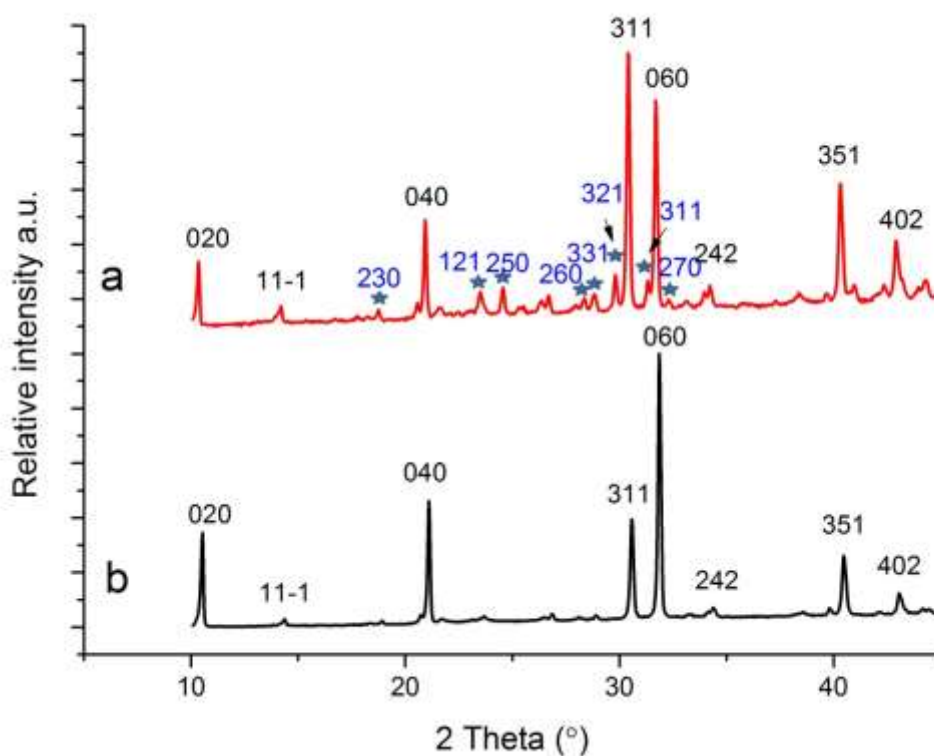


Figure 4. PXRD patterns of (a) samples taken 1 min after ethanol precipitation, where these contain many needle-like crystals. The peaks labelled with a blue star correspond to anhydrous KFC (orthorhombic) and black labelled peaks correspond to the trihydrate, KFCT (monoclinic or tetragonal), without preferred orientation (b) PXRD pattern of a sample taken 3 min after ethanol precipitation, comprising a mixture of hexagonal (higher proportion) and rectangular crystals with preferred orientation (060) due to platy shape of crystals.

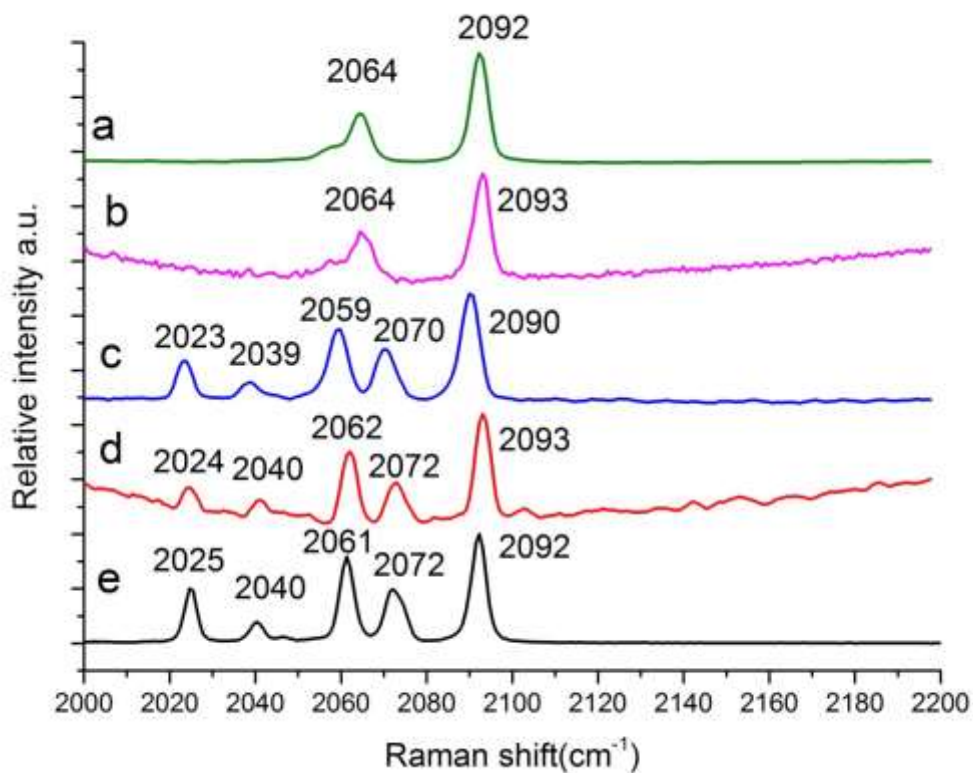


Figure 5. Raman spectra of the (a) rectangular, (b) octagonal and (c) hexagonal-shaped crystals of KFCT, and (d) the needle-shaped crystals in solution or (e) after heating KFCT at 200° for 2h which correspond to anhydrous KFC.

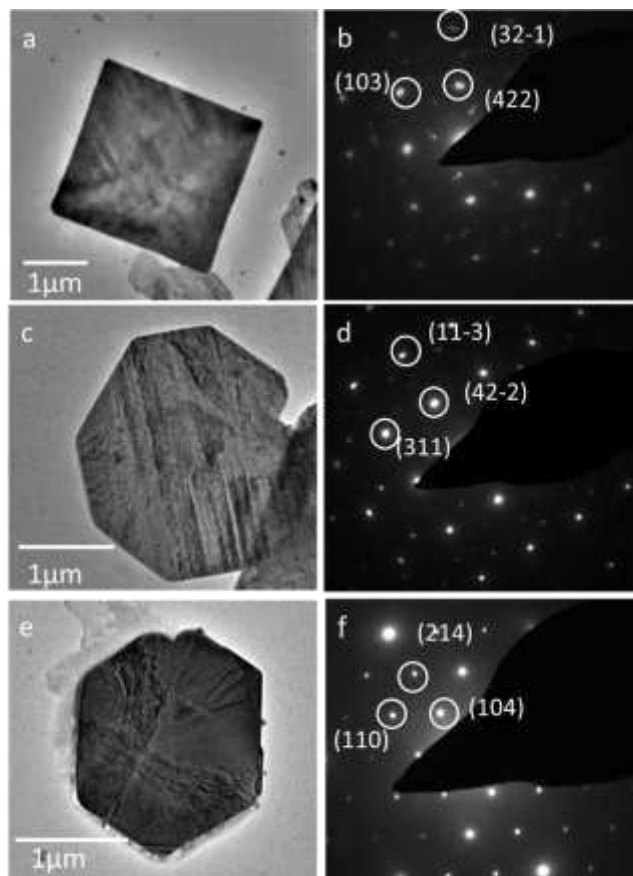


Figure 6. TEM images and corresponding selective area electron diffraction patterns of KFCT crystals. (a) A rectangular prism showing a monoclinic diffraction pattern (b), (c) an octagonal crystal showing a monoclinic diffraction pattern (d) and (e) a hexagonal crystal with a tetragonal diffraction pattern (f).

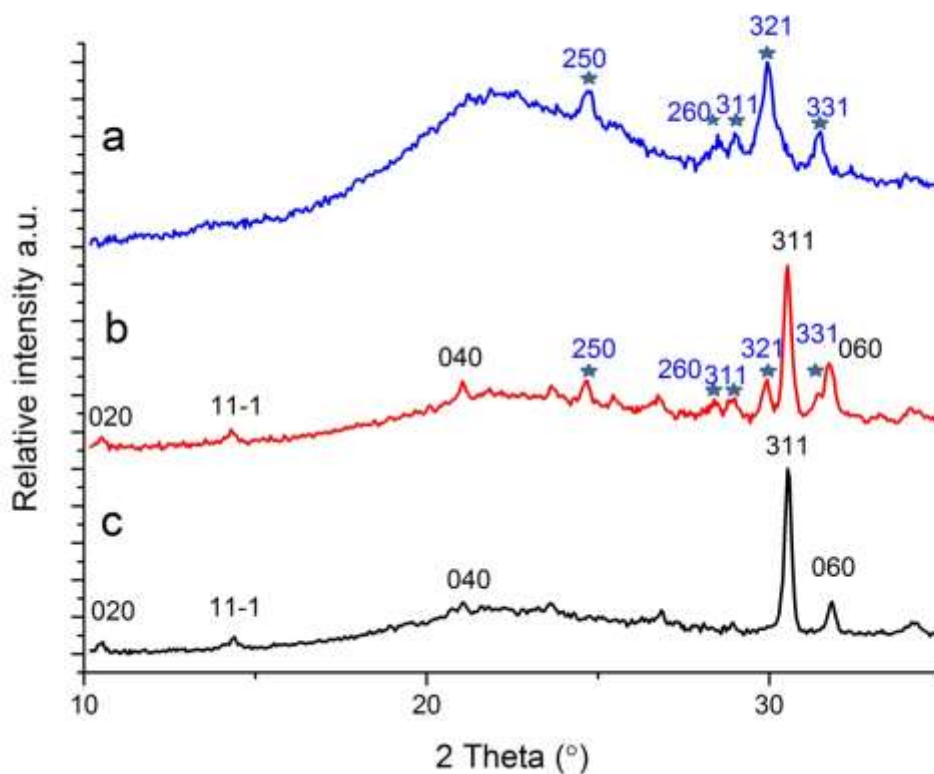


Figure 7. XRD patterns of crystals precipitated within CPG-362 particles after different evaporation times. Peaks from the anhydrous KFC are indicated in blue, while the KFCT peaks are labelled in black. (a) At $t < 24$ h only KFC was observed, (b) at 24 – 48 h, mixtures of KFC and KFCT crystals were found (we could not distinguish between polymorphs by PXRD) and (c) after 1 month, the pores contained KFCT only.

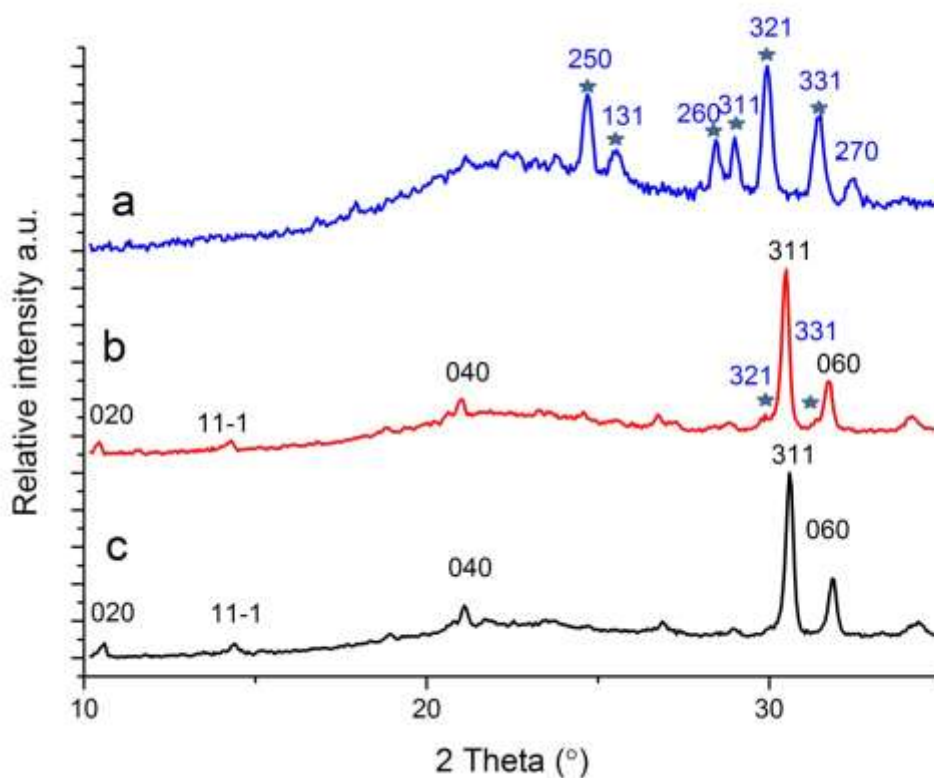


Figure 8. PXRD patterns of crystals precipitated within CPG-48 particles after different evaporation times. Peaks from the anhydrous KFC are labelled in blue while KFCT peaks are labelled in black. (a) At times < 24 h only KFC was observed, (b) at 24 – 48 h, mixtures of KFC and KFCT were found and (c) after 1 month, the pores contained KFCT only.

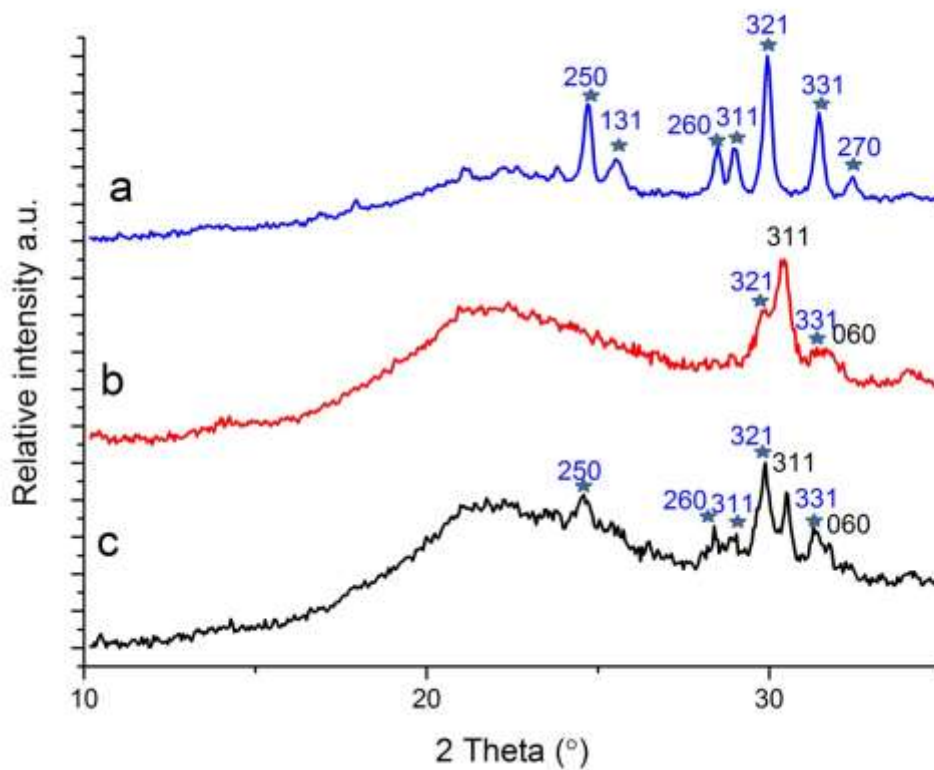


Figure 9 PXRD patterns of crystals precipitated within CPG-8 particles after different evaporation times. Peaks from the anhydrous KFC are labelled in blue, while KFCT peaks are labelled in black. (a) At times < 24 h only KFC was observed, (b) at 24 – 48 h, mixtures of KFC and KFCT crystals were found and (c) after 1 month, the pores still contained a mixture of KFC and KFCT.

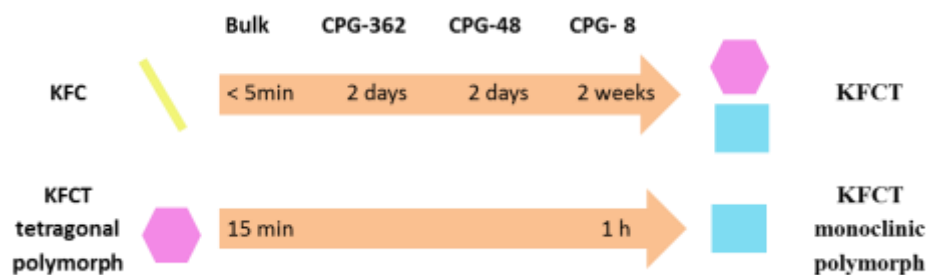


Figure 10. Crystal transformations that occur in bulk and in the CPGs under humid conditions. (a) KFC crystals precipitated in CPGs by vacuum drying transformed to a mixture of polymorphs of KFCT after 2 days in CPG-362 and CPG-48 nm and after 2 weeks in CPG-8 nm. By comparison, KFC crystals collected from bulk transformed in under 5 min. (b) KFCT tetragonal crystals isolated from bulk solution transformed into the stable monoclinic polymorph after 15 min, but in CPG-8 did not transform for 1 h.

FOR TABLE OF CONTENTS USE ONLY

Effect of Nanoscale Confinement on the Crystallization of Potassium Ferrocyanide

Clara Anduix-Canto¹, Yi-Yeoun Kim¹, Yunwei Wang¹, Alex N. Kulak¹, Fiona C. Meldrum^{1†}
and Hugo K. Christenson^{2*}



SYNOPSIS

Remarkable effects of confinement are seen on crystallizing potassium ferrocyanide in nanoporous glasses. The anhydrous salt, which is not observed in bulk, precipitates in the pores despite a large excess of water, and a metastable trihydrate persists »100 times longer than in bulk. Confinement clearly has a very general and significant effect on precipitation pathways and polymorph selection of crystals.